

# DESIGN AND MICROFABRICATION OF HIGH PERFORMANCE SUPER-LYOPHOBIC SURFACES

Tianzhun Wu, Yuji Suzuki and Nobuhide Kasagi

*Department of Mechanical Engineering, The University of Tokyo, Japan*

## ABSTRACT

We propose a systematic design method of super-lyophobic surfaces (SLS) showing extreme low wettability for any liquid for the first time. Design criteria including suspension and pinning conditions and equilibrium stability are essential for SLS. We demonstrate advantages of MEMS technologies for high performance SLS with highly-uniform overhang structures. High contact angle up to 159° and low contact angle hysteresis of 8° have been achieved both for water and hexadecane as well as high robustness and low adhesion.

**KEYWORDS:** Super-lyophobic, Cassie-Baxter state, Design criteria, MEMS

## INTRODUCTION

Although super-hydrophobic surfaces with high contact angle (CA) and low contact angle hysteresis (CAH) for water have attracted much attention for long time, they are not repellent to low surface tension liquids like oil. There are few oleophobic (oil-repellent) surfaces reports mainly due to lack of knowledge for oleophobicity mechanisms. Actually, most of oleophobic surfaces reported are fabricated using random nanostructures, usually suffered from uncontrollable performance and poor reproducibility. Not until recently Tuteja et al. [1,2] and Ahuja et al. [3] successfully fabricated super-lyophobic surfaces (SLS) showing high CA and low CAH for various liquids. However, systematic design rules of SLS are not established. Here, we propose the design criteria for high performance SLS by MEMS approaches, and systematically evaluate its performance for water and oil.

## DESIGN

According to the Cassie-Baxter (C-B) model, the equilibrium CA on air trapped surfaces is expressed as  $\cos \theta_{CB} = r_f f_s \cos \theta_{flat} + f_s - 1$ , where  $\theta_{CB}$  and  $\theta_{flat}$  are respectively static/dynamic CA on C-B and flat surfaces,  $r_f$  is roughness of wetted solid, and  $f_s$  is wetted solid fraction. To achieve the C-B state for liquid with low surface tension, the *suspending condition* must be satisfied;  $P_{up} > P_{down}$  and  $\lambda > H$ , where  $P_{up}$  is the maximum Laplace pressure produced by liquid curvature on the cavities, and  $P_{down}$  the imposed pressure such as gravity (Fig. 1).  $\lambda$  and  $H$  are respectively the liquid and the cavity height. To satisfy these conditions for oil, overhang structures with small overhang angle  $\theta_0$  (the angle between the solid curvature tangent and the horizontal) is essential [4]. Two basic overhang structures with sharp edges or curvatures are shown in Figs. 1ab. In addition,  $\theta_0$  should satisfy the second criteria called *pinning condition*. In equilibrium, the three phase contact line is pinned on corners or curvature, expressed as  $\theta_{pin}^{CB} \leq \theta_a^{CB}$ . In this inequality,

$\theta_{pin}^{CB}$  is the pinning CA on the C-B state as a function of  $f_s, \theta_0, P_{up}$  and  $P_{down}$ , while  $\Theta_a^{CB}$  is the maximum pinning CA on C-B state. The third criterion is *stable equilibrium* requirement for pinning so that liquid free energy is at local minimum. A simple expression given by [4] is  $\Delta A_{st} \Delta \theta_0 < 0$ , where  $A_{st}$  is the wetted solid area.

Based on these design criteria, we have chosen a T-shape overhang structure (or nail-shape) as a robust SLS structure, in which  $\theta_0=0$  for lower corner, thus any liquid can be pinned at the corners. Liquid with high surface tension ( $\gamma_{lv}$ ) pins on the upper corner (Fig. 1c) due to  $\theta_{pin}^{CB} \sim \pi < \Theta_a^{CB}$ , while liquid with low  $\gamma_{lv}$  depins from the upper corner since  $\theta_{pin}^{CB} \sim \pi > \Theta_a^{CB}$ , but pins on the lower corner (Fig. 1d) given  $\pi/2 < \theta_{pin}^{CB} < \Theta_a^{CB}$ . Thus C-B state can be achieved for any liquid.

### MEMS FABRICATION

Two MEMS fabrication methods are employed for proposed T-shape overhang structures for robust SLS surfaces.

Firstly, we pattern thermally grown SiO<sub>2</sub> on Si substrate using standard lithography. Then, Si pillars with the SiO<sub>2</sub> caps are formed with undercuts by XeF<sub>2</sub> non-plasma etching or deep reactive ion etching (DRIE). Finally conformal fluorocarbon (C<sub>x</sub>F<sub>y</sub>) is deposited

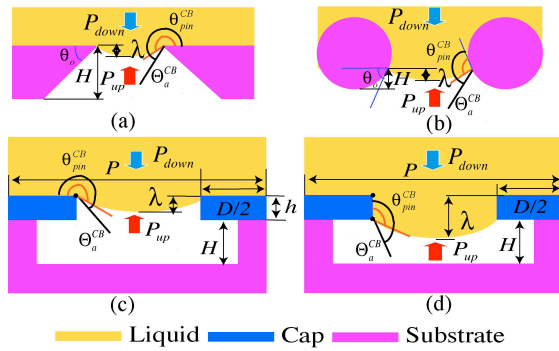


Figure 1. Design criteria for SLS. (a) Pinning on sharp edges, (b) Pinning on curvatures, (c) Pinning on T-shape upper corners, (d) Pinning on T-shape lower corners.

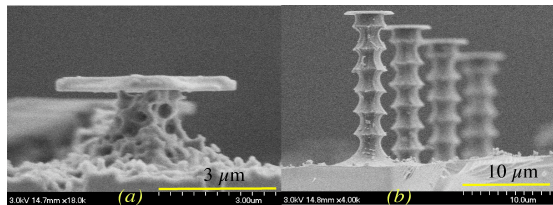


Figure 2. SEM of overhang structures. (a) Si pillars etched with XeF<sub>2</sub> (b) Si pillars etched with DRIE.

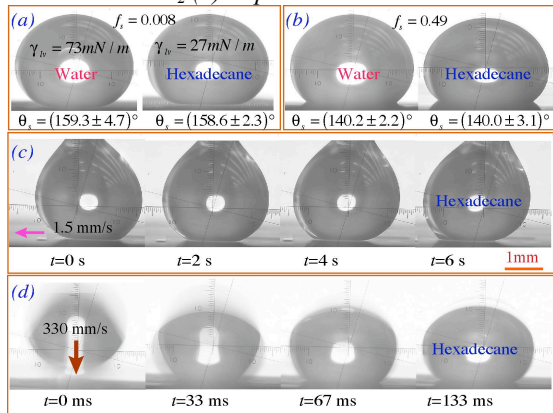


Figure 3. Images of DI water and hexadecane droplets on SLS. (a)  $P=50 \mu\text{m}, D=5 \mu\text{m}, H=36 \mu\text{m}$  (b)  $P=10 \mu\text{m}, D=7 \mu\text{m}, H=5 \mu\text{m}$  (c), (d)  $P=20 \mu\text{m}, D=6 \mu\text{m}, H=18 \mu\text{m}$ .

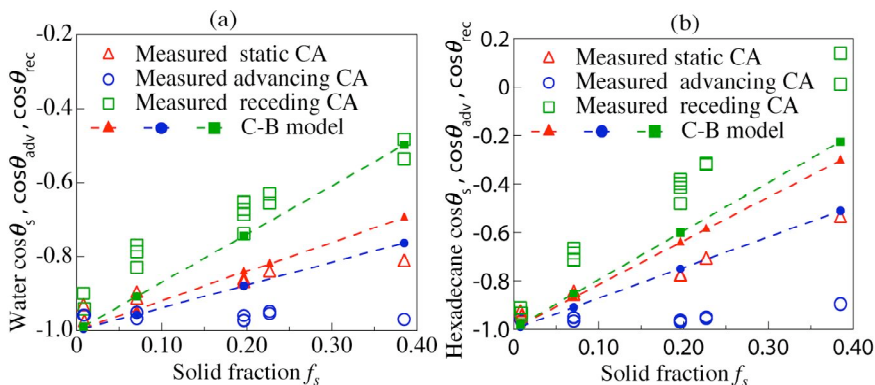


Figure 4. Static CA ( $\cos\theta_s$ ) and Dynamic CA ( $\cos\theta_{adv}$  and  $\cos\theta_{rec}$ ) in comparison with the C-B model prediction. (a) water, and (b) hexadecane.

using  $C_4F_8$  plasma.

## RESULTS AND DISCUSSION

Highly-uniform overhang structures have been achieved by both methods (Fig. 2) with different pitch  $P$ , cap diameter  $D$ , etching depth  $H$  and pattern layout. Si pillars with DRIE have smaller undercuts and much larger etching depth. Equilibrium CAs for water and hexadecane are as high as  $159^\circ$  (Fig. 3a). Advancing and receding CAs  $\theta_{adv}$  and  $\theta_{rec}$  are measured by slowly moving the substrate horizontally, while the droplet is fixed by a syringe (Fig. 3c). With  $f_s=0.008$  (Fig. 3a),  $\theta_{adv}=163^\circ$  and  $\theta_{rec}$  are respectively  $154^\circ$  and  $156^\circ$  for water and hexadecane, yielding  $\Delta\theta\sim 8^\circ$ . Oscillation of droplets by environmental vibration are also observed due to extreme low adhesion of SLS. Figure 3d shows the impact of a  $\sim 17\ \mu\text{L}$  hexadecane droplet released from  $\sim 9\ \text{mm}$  height, indicating robust lyophobicity even for oil.

Figures 4 shows that experimental data of  $\cos\theta_s$ ,  $\cos\theta_{adv}$  and  $\cos\theta_{rec}$  for water and hexadecane are almost linearly dependent on  $f_s$ . The present data for water are in reasonable agreement with the C-B model prediction for  $\theta_s$  and  $\theta_{rec}$ . However, the C-B model fails for  $\theta_{adv}$  of water and for all CAs of hexadecane. Therefore, a new wetting theory to explain droplet behavior is necessary for SLS.

## CONCLUSIONS

We have proposed the systematic design criteria for high performance SLS using MEMS approaches for the first time, and successfully microfabricated highly uniform overhang structures. High CA  $\sim 159^\circ$ , low CAH  $\Delta\theta\sim 8^\circ$ , low adhesion, and high robustness have been achieved for both water and hexadecane.

## REFERENCES

- [1] A. Tuteja et al., *Science*, **318**, 1618 (2007).
- [2] A. Tuteja et al., *PNAS*, **105**, 18200 (2008).
- [3] A. Ahuja et al., *Langmuir*, **24**, 9 (2008).
- [4] M. Nosonovsky et al., *Ultramicroscopy*, **107**, 969 (2007).